Journal of Materials Chemistry A

Accepted Manuscript

This is an *Accepted Manuscript*, which has been through the Royal Society of Chemistry peer review process and has been accepted for publication.

Accepted Manuscripts are published online shortly after acceptance, before technical editing, formatting and proof reading. Using this free service, authors can make their results available to the community, in citable form, before we publish the edited article. We will replace this *Accepted Manuscript* with the edited and formatted *Advance Article* as soon as it is available.

You can find more information about *Accepted Manuscripts* in the Information for Authors.

Please note that technical editing may introduce minor changes to the text and/or graphics, which may alter content. The journal's standard Terms & Conditions and the Ethical guidelines still apply. In no event shall the Royal Society of Chemistry be held responsible for any errors or omissions in this *Accepted Manuscript* or any consequences arising from the use of any information it contains.

ROYAL SOCIETY OF CHEMISTRY

www.rsc.org/materialsA

Journal of Materials Chemistry A RSCPublishing

ARTICLE

Cite this: DOI: 10.1039/x0xx00000x

Received 00th January 2012, Accepted 00th January 2012

DOI: 10.1039/x0xx00000x

www.rsc.org/

Plasma enhanced atomic layer deposition of Ga_2O_3 thin films

Ranjith K. Ramachandran[a], Jolien Dendooven[a], Jonas Botterman[b], Sreeprasanth Pulinthanathu Sree[c], Dirk Poelman[b], Johan A. Martens[c], Hilde Poelman[d] and Christophe Detavernier[a]*

Amorphous Ga_2O_3 thin films have been grown on SiO_2/Si substrates by atomic layer deposition (ALD) using tris (2,2,6,6-tetramethyl-3,5-heptanedionato) gallium(III) [$Ga(TMHD)_3$] as a gallium source and O_2 plasma as reactant. A constant growth rate of 0.1 Å/cycle was obtained in a broad temperature range starting from 100 to 400 °C. X-ray photoelectron spectroscopy (XPS) analysis revealed stoichiometric Ga_2O_3 thin films with no detectable carbon contamination. A double beam - double monochromator spectrophotometer was used to measure the transmittance of Ga_2O_3 thin films deposited on a quartz substrate and analysis of the adsorption edge yielded a band gap energy of 4.95 eV. The refractive index of the Ga_2O_3 films was determined from spectroscopic ellipsometry measurements and found to be 1.84 at a wavelength of 632.8 nm. Atomic force microscopic (AFM) analysis showed surface roughness values of 0.15 and 0.51 nm for films deposited at 200 and 400 °C, respectively. Finally, all the films could be crystallized into a monoclinic β-Ga_2O_3 crystal structure by a post deposition annealing in He as indicated by X-ray diffraction (XRD) measurements.

Introduction

Gallium oxide exists in several crystalline forms, of which the monoclinic (β-Ga_2O_3) phase has attracted much attention in recent years. Its very high thermal and chemical stability, along with the temperature dependent conducting behavior[1] makes it an important material in gas sensing applications. For example, at high temperatures (800-1000°C) the films can be used as oxygen sensors[2–6] while at lower temperatures (< 700°C) they are suitable for sensing reducing gases.[7–9] With a wide band gap of 4.9 eV, Ga_2O_3 exhibits conductive and photoluminescent[10–12] properties, rendering it a promising candidate for applications such as transparent conducting material[13–16] in next generation optoelectronic devices and deep-UV photodetectors.[17,18] The value of the refractive index close to the square root of the refractive index of GaAs allows it to be used as an efficient single-layer antireflection coating for GaAs.[19–21] Ga_2O_3 has also been used in catalytic[22,23] and photocatalytic[24] applications. Moreover gallium doped zinc oxide (Ga: ZnO) has become one of the most important candidates for TCO applications[25,26].

Currently, there are several methods employed for gallium oxide thin film deposition including sol-gel synthesis,[4,22,24,27] spray pyrolysis,[10,28] electron beam evaporation,[20,21,29] pulsed laser deposition,[12–15,30,31] sputter deposition,[2,3,5–9,32] molecular beam epitaxy (MBE),[16,17] chemical vapour deposition (CVD),[33–37] and atomic layer deposition (ALD).[38–49] Among them, ALD is one of the most promising, allowing one to obtain highly conformal materials with excellent thickness uniformity and composition control. There have been many efforts to obtain conformal ALD-Ga_2O_3 films using various precursors. The first successful ALD process for Ga_2O_3 was demonstrated by Nieminen et al.[38] employing $Ga(acac)_3$ and either water or ozone, but relatively high deposition temperatures (> 370°C) were required and an acceptable composition was only obtained with ozone. Among the processes that use amine-based precursors, the $Ga_2(NMe_2)_6$ and water process[40] has a narrow temperature window (170-250 °C), while the process that uses $[(CH_3)_2GaNH_2]_3$ and O_2 plasma[39,41,42,49] is limited to a working temperature of 200°C. Similarly, isopropoxide precursors are also limited by a narrow temperature window (280 - 300 °C[43] and 150 –

[a]Department of Solid State Sciences, CoCooN, Ghent University, Krijgslaan 281/S1, 9000 Ghent, Belgium,
E-mail: Christophe.detavernier@ugent.be, Phone: +32 9 264 4354, Fax: +32 9 264 4996
[b]Department of Solid State Sciences, LumiLab, Ghent University, Krijgslaan 281/S1, 9000 Ghent, Belgium
[c]Centre for Surface Chemistry and Catalysis, Catholic University of Leuven, Kasteelpark Arenberg 23, B-3001 Leuven, Belgium
[d]Laboratory for Chemical Technology, Ghent University, Technologiepark 914, B-9052 Zwijnaarde, Belgium

Journal of Materials Chemistry A Accepted Manuscript

250 °C[46]). Trimethyl gallium (TMGa) was recently introduced as a promising precursor for ALD of Ga_2O_3 in combination with ozone[44] or O_2 plasma.[47] Especially the plasma-activated process exhibits a wide temperature window, enabling the deposition of Ga_2O_3 films with a growth rate of 0.53 Å/cycle at temperatures as low as 100 °C.[47]

In this work, we use a beta-diketonate precursor, tris (2,2,6,6-tetramethyl-3,5-heptanedionato)gallium(III), $[Ga(TMHD)_3]$ as a gallium source and O_2 plasma as reactant. This process exhibits a broad temperature window (100 to 400 °C) similar to the TMGa and O_2 plasma process. Even though the growth rate of the novel process is lower (0.1 Å/cycle), this could be beneficial for doping applications where the concentration of the dopant has to be precisely controlled.[25,26] Additional advantages are its low cost, non-toxicity, and ease of handling. Moreover, it is worth mentioning that the beta-diketonate precursor has an enhanced volatility and thermal stability compared to the acetylacetone parent derivative induced by the replacement of the methylsubstituents on the acac ligands with tert-butyl groups.[50,51] As oxygen source, we tested H_2O, O_3 and O_2 plasma and found that only O_2 plasma resulted in successful deposition of gallium oxide. Hardly any growth was observed by performing 200 ALD cycles using H_2O or O_3 as reactant at a deposition temperature of 300 °C. On the other hand, the introduction of plasma during the ALD process enabled the deposition of high quality thin films at low temperatures.

Experimental details

All the depositions were performed on Si substrates covered with 100 nm thermally grown SiO_2 (SiO_2/Si) in a home-built pump type ALD reactor[50,51] with an operating base pressure of below 5×10^{-6} mbar. The chamber wall was heated to 150 °C. The solid $Ga(TMHD)_3$ precursor (99%, Strem Chemicals), kept in a stainless steel container, was heated to 135 °C, and the delivery line to the chamber was heated to 138 °C. For the remote plasma process the O_2 gas flowed through the plasma source at a pressure of 0.03 mbar and the RF plasma power was set at 300 W. The precursor was injected through a quarter inch stainless steel tube located at the top of the ALD chamber. Unless stated otherwise, the pulse times were 5 s for both the $Ga(TMHD)_3$ precursor and O_2 plasma. No purge gas was used in the deposition cycle.

The thickness of the growing Ga_2O_3 films was monitored in situ using spectroscopic ellipsometry (SE, J. A. Woollam M-2000). A Cauchy model was applied for fitting the ellipsometric data to obtain the film thickness and optical properties. The determination of film thickness by in situ SE was complemented by ex situ X-ray reflectivity (XRR) measurements. XRR was carried out using a Bruker D8 Discover system with Cu Kα radiation. X-ray fluorescence (XRF) measurements were performed using a Mo X-ray source (at an angle of 45° with sample surface) and a silicon drift detector placed at an angle of 52° with the sample surface. The fluorescence signal was integrated over a period of 100 s. The chemical composition of the deposited films was determined by X-ray photoelectron spectroscopy (XPS) using a Thermo VG Scientific ESCALAB 220i-XL with a monochromatic Al Kα x-ray source. The reported Binding Energy values (BE) were corrected for charging effects by assigning a BE of 284.6 eV to the C1s signal. The film crystallinity was investigated by X-ray diffraction (Bruker D8 Discover, Cu Kα radiation). The surface roughness of the films was determined by atomic force microscopy (AFM) on a Bruker Dimension Edge system operating in tapping mode in air. The Root Mean Square (RMS) roughness values were calculated on 5 µm x 5 µm micrographs. To measure the transmittance, a 10 nm thick Ga_2O_3 film was deposited on a quartz substrate. The optical transmittance at normal incidence was measured with a double beam – double monochromator UV-VIS-NIR spectrophotometer (Cary 500, Varian, USA) in the UV-visible range (200–600 nm).

The ALD process was characterized by in situ quadrupole mass spectrometry (QMS, Hiden Analytical) using the spectrometer in Multiple Ion Detection (MID) mode with the Faraday detector (source voltage 70 V).

Finally, post-annealing of the deposited films in He was performed in a home-built heating chamber mounted on a Bruker D8 diffractometer[52,53] to enable *in situ* XRD characterization. A linear detector was used to collect the diffracted X-rays at 2 s time intervals.

Results and discussion

Characteristics of the Gallium Oxide ALD process

The temperature window of the ALD process was investigated on Si substrates covered with 100 nm thermally grown SiO_2. Depositions were carried out over a wide temperature range from 75 to 400 °C. Figure 1 shows the variation in growth per cycle (GPC) with the temperature of the substrate. A constant growth rate of 0.1 Å per cycle was obtained within a temperature window ranging from 100 to 400 °C. This broad temperature window could be of interest for doping applications, where the deposition temperatures for different ALD processes have to overlap.[25,26] A higher growth rate was observed below 100 °C, probably due to condensation of the precursor onto the substrate or the incomplete removal of the reaction by-products at low temperatures causing some organic residues from the precursor ligands to become incorporated into the film. The temperature stability of the $Ga(TMHD)_3$ precursor at higher temperature was also tested. For this, a SiO_2/Si substrate and an ALD grown Ga_2O_3 film were placed on the sample holder at 400 °C. Then the precursor alone was pulsed into the reactor without O_2 plasma half cycle. No thickness increase was found even after 300 precursor pulses, confirming that no decomposition of the precursor occurred at 400 °C.

Saturation of the ALD half-cycles was studied on SiO_2/Si substrates at a deposition temperature of 200 °C. Figure 2 shows the saturation curves for the $Ga(TMHD)_3$ precursor (triangles) and O_2 plasma (circles) half cycles respectively. First, the pulse time of the $Ga(TMHD)_3$ precursor was varied while keeping a constant O_2 plasma exposure of 5s. The experiments showed that a pulse time of 4s, at a pressure of 3×10^{-3} mbar in the chamber, was sufficient to reach saturated growth. Similar experiments were then performed for the O_2 plasma step and the saturation of the growth per cycle was achieved at an O_2 plasma pulse time of 2 s.

Journal of Materials Chemistry A Accepted Manuscript

This journal is © The Royal Society of Chemistry 2012

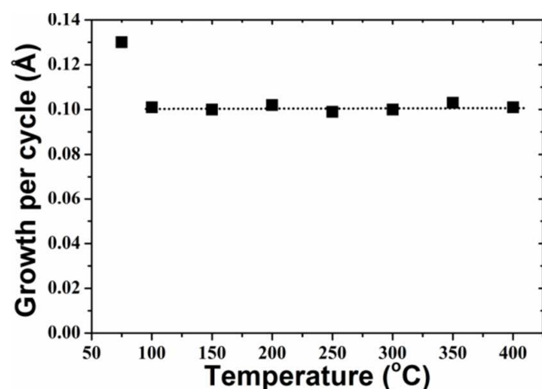

Figure 1. Growth rate as a function of deposition temperature. The dotted line serves as a guide to the eye.

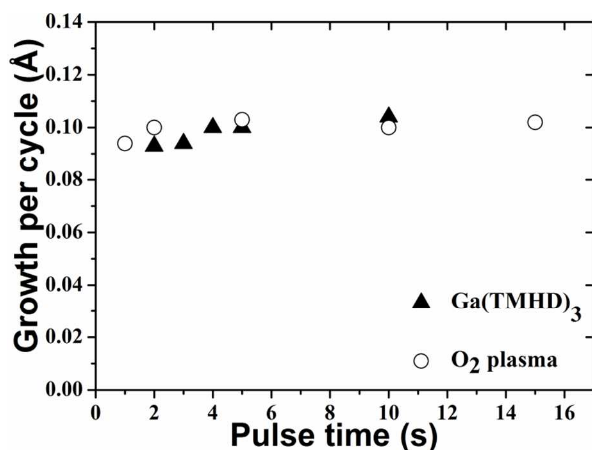

Figure 2. Growth per cycle against the $Ga(TMHD)_3$ pulse time (triangles), using a fixed O_2 plasma exposure of 5 s and growth per cycle against the O_2 plasma exposure time (circles), using a fixed $Ga(TMHD)_3$ pulse time of 5s at 200 °C.

To get more insights into the mechanisms of this novel process, in situ QMS was used to analyze the reaction products formed during both ALD half cycles. The surface reaction kinetics of adsorbed metal β-diketonate precursors with O radicals has been studied extensively by T.T. Van and J.P. Chang.[54,55] According to the mechanism described in their work, the incoming $Ga(TMHD)_3$ molecules are expected to adsorb non-dissociatively on the surface during the precursor pulse. In the subsequent O_2 plasma pulse, O radicals will react with the organic β-diketonate ligands, likely leading to the formation of non-volatile metal oxide and volatile CO and CO_2. This type of ligand combustion mechanism is common in plasma enhanced ALD processes using any kind of organometallic precursors[56–59]. To analyze the formation of reaction products during the $Ga(TMHD)_3/O_2$ plasma process a series of QMS measurements in MID mode were performed. In the same scan 5 precursor pulses (A) were monitored, followed by 3 full ALD cycles (i.e. precursor and reactant pulse (AB)) and finally 5 reactant pulses (B). The sequence monitored is thus: AAAAA ABABAB BBBBB. During the successive precursor pulses (A) and successive reactant pulses (B), no reactions occur, so a clean precursor (A) or reactant (B) signal is obtained for the different mass-to-charge ratios that are being monitored. By comparing these reference signals with the precursor and reactant signal during the ALD cycles (AB), the formation of reaction products can be interpreted. A series of relevant mass-to-charge ratios was followed during the scan, however, the only reaction products that could be detected were CO (m/z = 28) and CO_2 (m/z = 44). The QMS data recorded during the fifth precursor pulse (A), the three complete ALD cycles (ABABAB) and the next two O_2 plasma (B) pulses are shown in the figure 3. It can be seen that similar QMS signals are obtained during both the pure precursor pulse (A) and the precursor pulse in the ALD cycle (AB), which indicates that no gaseous reaction products can be detected during the precursor half cycle and that the precursor molecules indeed adsorb non-dissociatively on the surface. After pumping out the reaction products, oxygen plasma was introduced and the partial pressure of both CO_2 and CO increased. As oxygen -

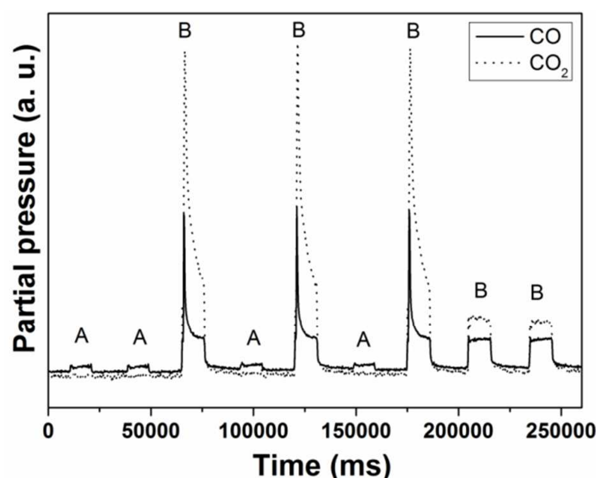

Figure 3. In situ mass spectrometry results for CO (m/z = 28) and CO_2 (m/z = 44) during different precursor (A) and reactant (B) pulses.

plasma continued to be dosed, both reaction product signals decreased, meaning that the reaction approached completion. The sharp spike in the MID signal was not observed during the pure O_2 plasma (B) pulse, indicating that the detected formation of CO_2 and CO during the O_2 plasma (B) pulse of the ALD cycle (AB) can be attributed the reaction of O radicals with the adsorbed precursor molecules. The results obtained from our experiment are therefore consistent with the observations in the above mentioned references.[54,55]

Linearity of the ALD process at 200 °C was verified on SiO_2/Si substrates. Figure 4 shows that the film thickness depends linearly on the number of reaction cycles without any nucleation delay, that is, the growth rate remains constant throughout the process.

Properties of the Gallium Oxide Films

Gallium oxide films were deposited on 100 nm SiO_2/ Si substrates using the conditions described in the experimental section. All the deposited films were continuous and the thickness uniformity

Journal of Materials Chemistry A Accepted Manuscript

was excellent, with a typical deviation in thickness of less than 2% across a two-inch area. Phase identification of ca. 30 nm thick films was performed using XRD measurements. All the films were found to be amorphous in the as-deposited state irrespective of their deposition temperature. Upon annealing under He atmosphere, poly-

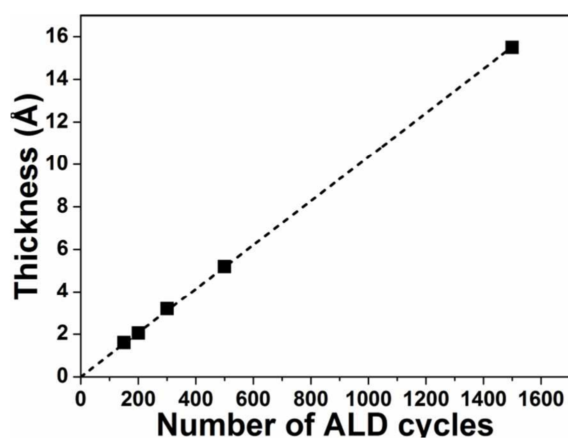

Figure 4. Thickness of the Ga_2O_3 films deposited at 200 °C on SiO_2/Si substrates against the number of ALD cycles.

crystalline β-Ga_2O_3 films with a monoclinic crystal structure were obtained. Figure 5 shows the XRD patterns for the as-deposited film at 200 °C and for the same film annealed in He to 900 °C at a heating rate of 0.2 °C/s. The inset of Figure 3 shows the evolution of the XRD pattern during this thermal treatment. Crystallization of the film started at 630 °C, as revealed by the intensification of the peak corresponding to β-Ga_2O_3 [(004), (-104)].

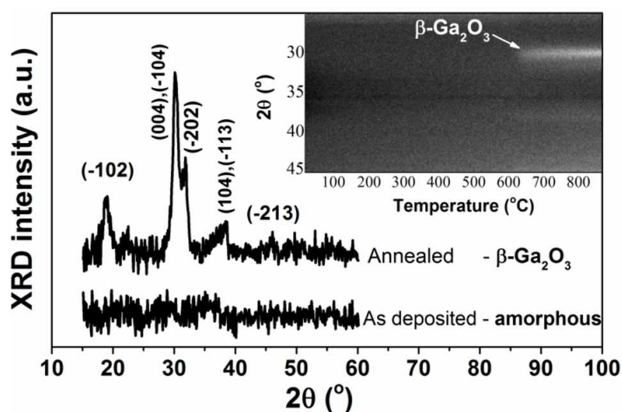

Figure 5. XRD patterns of a 30 nm thick Ga_2O_3 film deposited at 200 °C on a SiO_2/Si substrate and of the same film after annealing in He to 900 °C at a heating rate of 0.2 °C/s. The inset shows the evolution of the XRD pattern during this thermal treatment.

Chemical composition and bonding states of the deposited Ga_2O_3 thin films were studied by XPS. Figure 6 (a) shows the survey spectra collected for the film deposited on the SiO_2/Si substrate at 200 °C before and after sputtering in the XPS chamber. The spectra show relevant photoelectron peaks for gallium (Ga $2p_{1/2}$, Ga $2p_{3/2}$, Ga 3s, Ga 3p, and Ga 3d) and oxygen (O 1s, O 2s), together with the Auger lines from gallium (GaLMM) and oxygen (OKVV, OKLL).[33,43,60,61] The spectrum before sputtering showed surface contamination by carbon, but after the sputtering process, the carbon peak was not observed. The binding energies of the Ga $2p_{1/2}$ (1118.5 eV), Ga $2p_{3/2}$ (1145.5 eV) [Fig. 6(b)] and O 1s (531.5 eV) photoelectron peaks obtained from a high-resolution spectrum indicate that the gallium is in the 3+ oxidation state (Ga^{3+}). The Ga/O ratio (0.64) was found to be in agreement with the stoichiometry expected for Ga_2O_3. Comparing these observations with those reported in literature,[33,37,38,43,45,60–63] it can be concluded that the deposited films are Ga_2O_3.

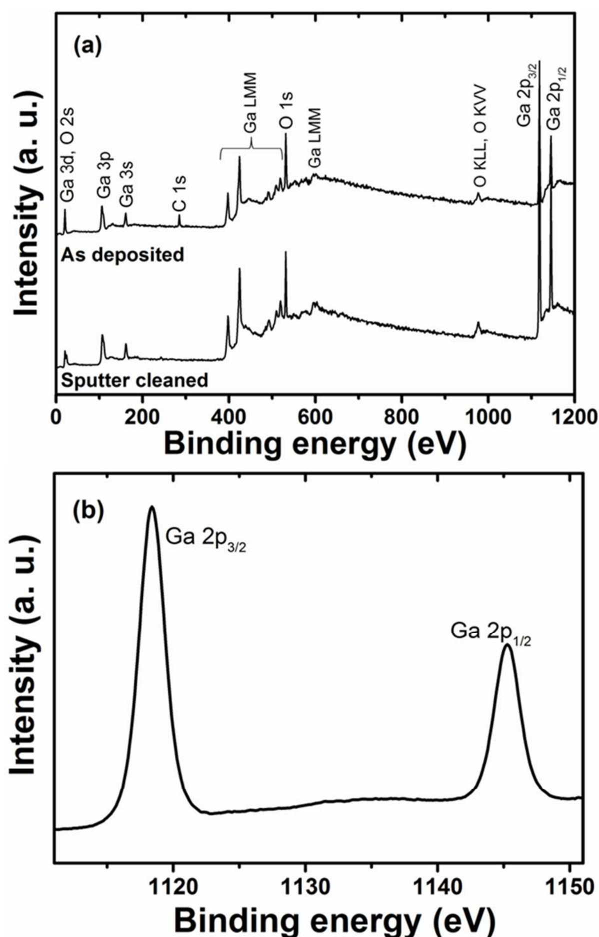

Figure 6. XPS spectra of a Ga_2O_3 film deposited at 200 °C. (a) Survey spectra and (b) high-resolution measurement of the Ga 2p peaks.

The optical properties of the as-deposited Ga_2O_3 films were determined using spectroscopic ellipsometry and optical transmittance measurements. The inset of Figure 7 shows the transmittance of a 10 nm thick (determined with XRR) Ga_2O_3 film deposited on a quartz substrate at 200 °C divided by the transmittance of the bare quartz substrate. The film shows a nearly 100% optical transmission in the visible region, which is an important property for applications of Ga_2O_3 as TCO material or as antireflection coating. To determine the band gap (E_g) of the material, the absorption coefficient α was calculated form the transmittance, T, and the film thickness, d, as -ln(T)/d. In Figure 7,

Journal of Materials Chemistry A Accepted Manuscript

 This journal is © The Royal Society of Chemistry 2012

$[\alpha(h\nu)]^2$ is plotted against the photon energy hν. Because β-Ga_2O_3 is a direct band gap material, the value of the optical band gap can be determined from this plot by interpolation of the linear fit to the absorption edge to zero.[49,64] As shown in Figure 7, this analysis yielded a value of 4.95 eV, in agreement with reported values in literature.[49,65]

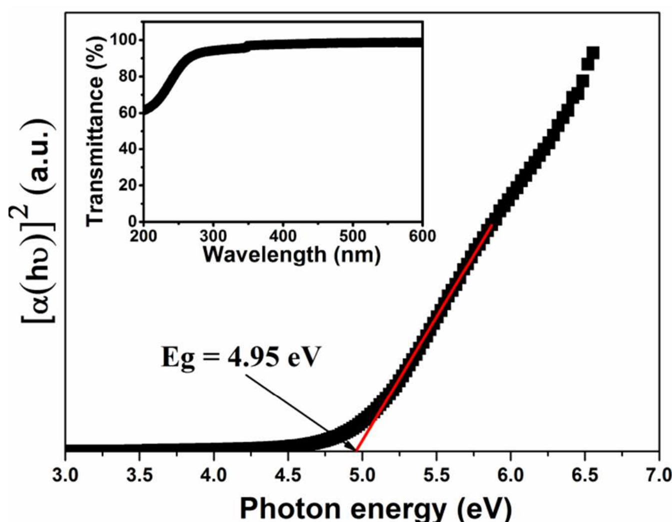

Figure 7. $[\alpha (h\nu)]^2$ versus photon energy plot for a 10 nm β-Ga_2O_3 film deposited on a quartz substrate at 200 °C. The band gap energy is determined from the linear fit (red line) to the absorption edge as indicated. The inset of the figure shows the transmittance spectrum of the same film divided by the transmittance of the bare quartz substrate.

In spectroscopic ellipsometry, the change in polarization of light upon reflection from a sample is described by an amplitude ratio, Ψ, and a phase difference, Δ, and is measured for a range of photon wavelengths (245 - 1200 nm). Figure 8 shows the Ψ (red line) and Δ (blue line) values measured for a 10.5 nm thick (determined with XRR) Ga_2O_3 film deposited on a SiO_2 substrate at 200 °C. From this data, the refractive index of the Ga_2O_3 film can be deduced through a fitting-based analysis. Because of the excellent transparency of the Ga_2O_3 film in the considered wavelength range, as revealed by the transmittance measurements, it is valid to use a Cauchy relation to model the refractive index of the Ga_2O_3 film: $n(\lambda) = A + B/\lambda^2 + C/\lambda^4$. As can be seen in Figure 8, an excellent fit (dashed black lines) is obtained for values of 1.805, 0.013 and 0.000442 for A, B and C respectively. The variation of refractive index (n) with the wavelength as obtained from the analysis is shown in the inset of figure 8. Independent of the deposition temperature, this fitting procedure yielded a refractive index value (n) of 1.84 at a wavelength of 632.8 nm, in agreement with literature values reported for Ga_2O_3 films prepared by other methods.[20,28,49]

The morphology of the films was studied using AFM (Figure 9). The films grown at low temperature (200 °C) were found to be very smooth (rms roughness ~ 1 – 2 Å), with a roughness that slightly increased during crystallization anneal (up to ~ 3 Å). Films grown at a higher temperature (400 °C) were slightly rougher as-deposited (rms roughness ~ 5 – 6 Å), but the roughness did not increase after crystallization. The rms roughness values obtained from the AFM analysis were in good agreement with the roughness estimated from XRR measurements. XRR analysis also revealed a roughness of ~ 3 – 4 Å for the Si or SiO_2 substrate after the deposition of Ga_2O_3, suggesting a smooth film/substrate interface.

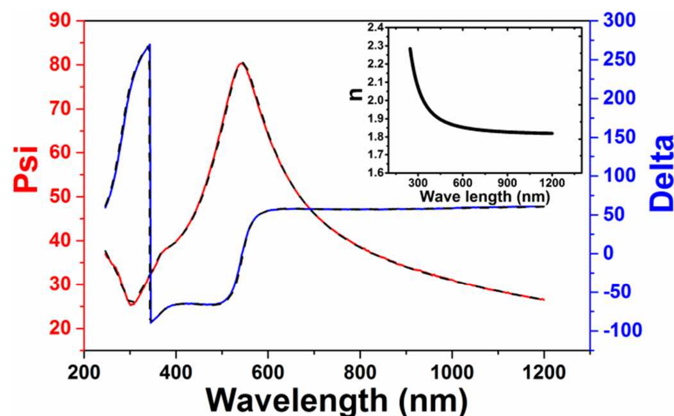

Figure 8. Ellipsometry signals Ψ (red line) and Δ (blue line) for a 10.5 nm Ga_2O_3 film deposited on a SiO_2 substrate at 200°C. The dashed lines are the Ψ and Δ curves generated by the Cauchy model. The inset shows the variation of refractive index (n) with wavelength.

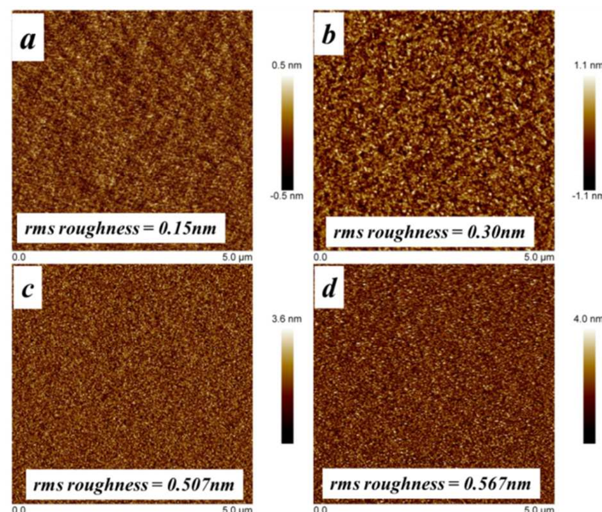

Figure 9. Atomic force micrographs of 30 nm thick Ga_2O_3 films deposited at 200 °C (a) before and (b) after crystallization, and at 400 °C (c) before and (d) after crystallization.

Finally, in view of applications where Ga_2O_3 thin films are needed on complex 3D substrates, e.g. large area nanostructured substrates for sensing or catalytic applications, the conformal nature of the novel PE-ALD process was verified. Ga_2O_3 was deposited in a mesoporous silica thin film with only 6 nm wide pores. Mesoporous films with fully accessible porosity was synthesized on Si supports using a reported procedure.[66] Ellipsometric porosimetry measurements showed that the silica film had a thickness of 150 nm, a porosity of 55% and a surface area of ca. 25 cm^2 per square

Journal of Materials Chemistry A Accepted Manuscript

centimeter of film. Because cross-sectional electron microscopy studies were found to be difficult for this type of porous films, the conformality was investigated by means of XRF.[56,67–70] The mesoporous film together with a planar SiO_2/Si reference was loaded into the deposition chamber and was heated to 200 ^oC. A long pulse time of 20 s was used for the $Ga(TMHD)_3$ to ensure the conformal coating into the pores. The O_2 plasma exposure time was 15 s. A series of depositions were performed by varying the number of ALD cycles. After the deposition the amount material deposited was determined by XRF measurements. The integrated area under the Ga Kα peak was then plotted against the number of ALD cycles (figure 10). Considerably more Ga_2O_3 was deposited in the mesoporous film during the first 200 ALD cycles, confirming conformal growth on the interior surface of the very small silica pores. From 250 ALD cycles, linear growth at a rate which is more similar to the growth on the planar reference is observed. This indicates that the small mesopores became inaccessible for the $Ga(TMHD)_3$ precursor and that growth continued on top of the coated mesoporous film.

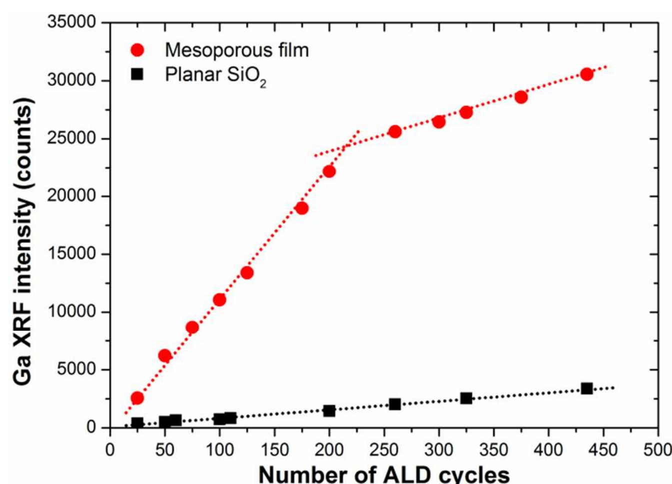

Figure 10. XRF growth curves for Ga_2O_3 ALD at 200 °C in a mesoporous silica thin film and on a planar SiO_2 substrate.

Conclusion

We have demonstrated a new process for the ALD of Ga_2O_3 thin films using tris (2,2,6,6-tetramethyl-3,5-heptanedionato) gallium(III) [$Ga(TMHD)_3$] as a gallium source and O_2 plasma as reactant. A constant growth rate of 0.1 Å/cycle was obtained in a broad temperature range starting from 100 to 400 ^oC. XPS studies confirmed the presence of Ga_2O_3. As-deposited films were found to be amorphous, while annealing in He resulted in the formation of β-Ga_2O_3 with monoclinic crystal structure. The refractive index and optical band gap of the material were determined to be 1.84 and 4.95 eV, respectively. Surface morphology studies of the films showed fairly smooth films (RMS roughness of 0.15 to 0.507 nm) with a slight increase in roughness upon annealing. Finally, Ga_2O_3 was deposited conformally in sub-10 nm silica mesopores, making this process attractive for the design of novel sensing and catalytic nanostructured surfaces.

Acknowledgements

This research was supported by the European Research Council (Starting Grant No. 239865), by the Flemish Research Foundation (FWO), the ‘Long Term Structural Methusalem Funding by the Flemish Government’ and by the Special Research Fund BOF of Ghent University (GOA 01G01513).

Notes and references

1 M. Fleischer and H. Meixner, *J. Appl. Phys.*, 1993, **74**, 300
2 M. Fleischer and H. Meixner, *Sensors Actuators B*, 1991, **5**, 115–119
3 M. Ogita, *Appl. Surf. Sci.*, 1999, **142**, 188–191
4 Y. Li, A. Trinchi, W. Wlodarski, K. Galatsis, and K. Kalantar-zadeh, *Sensors Actuators B*, 2003, **93**, 431–434
5 M. Ogita, S. Yuasa, K. Kobayashi, Y. Yamada, Y. Nakanishi, and Y. Hatanaka, *Appl. Surf. Sci.*, 2003, **212-213**, 397–401
6 C. Baban, Y. Toyoda, and M. Ogita, *Thin Solid Films*, 2005, **484**, 369–373
7 M. Fleischer, J. Giber, and H. Meixner, *Appl. Phys. A*, 1992, **54**, 560–566
8 O. Ring and D.Mllnchen, *Sensors Actuators B*, 1996, **34**, 378–382
9 M. Fleischer, S. Kornely, T. Weh, J. Frank, and H. Meixner, *Sensors Actuators B*, 2000, **69**, 205–210
10 J. Hao and M. Cocivera, *J. Phys. D*, 2002, **35**, 433–438
11 E. Nogales, J. a. García, B. Méndez, and J. Piqueras, *J. Appl. Phys.*, 2007, **101**, 033517
12 P. Wellenius, a. Suresh, and J. F. Muth, *Appl. Phys. Lett.*, 2008, **92**, 021111
13 M. Orita, H. Ohta, M. Hirano, and H. Hosono, *Appl. Phys. Lett.*, 2000, **77**, 4166–4168
14 M. Orita, H. Hiramatsu, H. Ohta, M. Hirano, and H. Hosono, *Thin Solid Films*, 2002, **411**, 134–139
15 K. Matsuzaki, H. Yanagi, T. Kamiya, H. Hiramatsu, K. Nomura, M. Hirano, and H. Hosono, *Appl. Phys. Lett.*, 2006, **88**, 092106
16 E. G. Víllora, K. Shimamura, K. Kitamura, and K. Aoki, *Appl. Phys. Lett.*, 2006, **88**, 031105
17 T. Oshima, T. Okuno, and S. Fujita, *Jpn. J. Appl. Phys.*, 2007, **46**, 7217–7220
18 S. Kumar and R. Singh, *Phys. status solidi*, 2013, **7**, 781–792
19 M. Taniguchi, T. Murakawa, and Y. Kajitani, *Appl. Surf. Sci.*, 1992, **56-58**, 827–831
20 M. Passlack, N. E. J. Hunt, E. F. Schubert, G. J. Zydzik, M. Hong, J. P. Mannaerts, R. L. Opila, and R. J. Fischer, *Appl. Phys. Lett.*, 1994, **64**, 2715
21 N. C. Oldham, C. J. Hill, C. M. Garland, and T. C. McGill, *J. Vac. Sci. Technol. A*, 2002, **20**, 809–813
22 M. Haneda, Y. Kintaichi, T. Mizushima, N. Kakuta, and H. Hideaki, *Appl. Catal. B*, 2001, **31**, 81–92
23 K.-J. Chao and P.-H. Liu, *Catal. Surv. from Asia*, 2005, **9**, 11–15
24 Y. Hou, L. Wu, X. Wang, Z. Ding, Z. Li, and X. Fu, *J. Catal.*, 2007, **250**, 12–18
25 W. J. Maeng and J.-S. Park, *J. Electroceramics*, 2013, **31**, 338–344
26 P. R. Chalker, P. a. Marshall, S. Romani, J. W. Roberts, S. J. C. Irvine, D. a. Lamb, A. J. Clayton, and P. a. Williams, *J. Vac. Sci. Technol. A*, 2013, **31**, 01A120

Journal of Materials Chemistry A Accepted Manuscript

 This journal is © The Royal Society of Chemistry 2012

27 T. Minami, T. Shirai, T. Nakatani, and T. Miyata, *Jpn. J. Appl. Phys.*, 2000, **39**, L524–L526
28 A. Ortiz, J. C. Alonso, E. Andrade, and C. Urbiola, *J. Electrochem. Soc.*, 2001, **148**, F26–F29
29 S. Pal, S. K. Ray, B. R. Chakraborty, S. K. Lahiri, and D. N. Bose, *J. Appl. Phys.*, 2001, **90**, 4103–4107
30 K. Matsuzaki, H. Hiramatsu, K. Nomura, H. Yanagi, T. Kamiya, M. Hirano, and H. Hosono, *Thin Solid Films*, 2006, **496**, 37–41
31 L. Nagarajan, R. a De Souza, D. Samuelis, I. Valov, A. Börger, J. Janek, K.-D. Becker, P. C. Schmidt, and M. Martin, *Nat. Mater.*, 2008, **7**, 391–398
32 S. S. Kumar, E. J. Rubio, M. Noor-A-Alam, G. Martinez, S. Manandhar, V. Shutthanandan, S. Thevuthasan, and C. V. Ramana, *J. Phys. Chem. C*, 2013, **117**, 4194–4200
33 G. a. Battiston, R. Gerbasi, M. Porchia, R. Bertoncello, and F. Caccavale, *Thin Solid Films*, 1996, **279**, 115–118
34 S. Bott, L. Miine, S. Suh, J. Liu, W. Chu, and D. Hoffman, *J. Mater. Chem.*, 1999, **9**, 929–935
35 M. Valet and D. M. Hoffman, *Chem. Mater.*, 2001, **13**, 2135–2143
36 H. W. Kim and N. H. Kim, *Appl. Surf. Sci.*, 2004, **230**, 301–306
37 S. Basharat, C. J. Carmalt, R. Binions, R. Palgrave, and I. P. Parkin, *Dalt. Trans.*, 2008, **9226**, 591–595
38 M. Nieminen, L. Niinisto, and E. Rauhala, *J. Mater. Chem.*, 1996, **6**, 27–31
39 N.-J. Seong, S.-G. Yoon, and W.-J. Lee, *Appl. Phys. Lett.*, 2005, **87**, 082909
40 C. L. Dezelah, J. Niinisto, K. Arstila, L. Niinisto, and C. H. Winter, *Chem. Mater.*, 2006, **18**, 471–475
41 F. K. Shan, G. X. Liu, W. J. Lee, G. H. Lee, I. S. Kim, and B. C. Shin, *Integr. Ferroelectr.*, 2006, **80**, 197–206
42 G. X. Liu, F. K. Shan, J. J. Park, W. J. Lee, G. H. Lee, I. S. Kim, B. C. Shin, and S. G. Yoon, *J. Electroceramics*, 2006, **17**, 145–149
43 H. Lee, K. Kim, J.-J. Woo, D.-J. Jun, Y. Park, Y. Kim, H. W. Lee, Y. J. Cho, and H. M. Cho, *Chem. Vap. Depos.*, 2011, **17**, 191–197
44 D. J. Comstock and J. W. Elam, *Chem. Mater.*, 2012, **24**, 4011–4018
45 A. K. Chandiran, N. Tetreault, R. Humphry-Baker, F. Kessler, E. Baranoff, C. Yi, M. K. Nazeeruddin, and M. Grätzel, *Nano Lett.*, 2012, **12**, 3941–3947
46 D. Choi, K.-B. Chung, and J.-S. Park, *Thin Solid Films*, 2013, **546**, 31–34
47 I. Donmez, C. Ozgit-Akgun, and N. Biyikli, *J. Vac. Sci. Technol. A*, 2013, **31**, 01A110
48 H. Altuntas, I. Donmez, C. Ozgit-Akgun, and N. Biyikli, *J. Vac. Sci. Technol. A*, 2014, **32**, 041504
49 F. K. Shan, G. X. Liu, W. J. Lee, G. H. Lee, I. S. Kim, and B. C. Shin, *J. Appl. Phys.*, 2005, **98**, 023504
50 Q. Xie, Y.-L. Jiang, C. Detavernier, D. Deduytsche, R. L. Van Meirhaeghe, G.-P. Ru, B.-Z. Li, and X.-P. Qu, *J. Appl. Phys.*, 2007, **102**, 083521
51 J. Musschoot, Q. Xie, D. Deduytsche, S. Van den Berghe, R. L. Van Meirhaeghe, and C. Detavernier, *Microelectron. Eng.*, 2009, **86**, 72–77
52 W. Knaepen, C. Detavernier, R. L. Van Meirhaeghe, J. Jordan Sweet, and C. Lavoie, *Thin Solid Films*, 2008, **516**, 4946–4952
53 W. Knaepen, S. Gaudet, C. Detavernier, R. L. Van Meirhaeghe, J. J. Sweet, and C. Lavoie, *J. Appl. Phys.*, 2009, **105**, 083532
54 T. T. Van and J. P. Chang, *Appl. Surf. Sci.*, 2005, **246**, 250–261
55 T. T. Van and J. P. Chang, *Surf. Sci.*, 2005, **596**, 1–11
56 R. K. Ramachandran, J. Dendooven, and C. Detavernier, *J. Mater. Chem. A*, 2014, **2**, 10662–10667
57 D. Longrie, K. Devloo-Casier, D. Deduytsche, S. Van den Berghe, K. Driesen, and C. Detavernier, *ECS J. Solid State Sci. Technol.*, 2012, **1**, Q123–Q129
58 I. J. M. Erkens, a. J. M. Mackus, H. C. M. Knoops, P. Smits, T. H. M. van de Ven, F. Roozeboom, and W. M. M. Kessels, *ECS J. Solid State Sci. Technol.*, 2012, **1**, P255–P262
59 S. M. George, *Chem. Rev.*, 2010, **110**, 111–31
60 M. Valet and D. M. Hoffman, *Chem. Mater.*, 2001, **13**, 2135–2143
61 D. H. Kim, S. H. Yoo, T. Chung, K. An, H. Yoo, and Y. Kim, *Bull. Korean Chem. Soc*, 2002, **23**, 225–228
62 G. Schon, *J. Electron Spectros. Relat. Phenomena*, 1973, **2**, 75–86
63 R. Carli and C. Bianchi, *Appl. Surf. Sci.*, 1994, **74**, 99–102
64 K. Prabakar, S. Venkatachalam, Y. . Jeyachandran, S. . Narayandass, and D. Mangalaraj, *Mater. Sci. Eng. B*, 2004, **107**, 99–105
65 K. Takakura, D. Koga, H. Ohyama, J. M. Rafi, Y. Kayamoto, M. Shibuya, H. Yamamoto, and J. Vanhellemont, *Phys. B Condens. Matter*, 2009, **404**, 4854–4857
66 S. P. Sree, J. Dendooven, D. Smeets, D. Deduytsche, A. Aerts, K. Vanstreels, M. R. Baklanov, J. W. Seo, K. Temst, A. Vantomme, C. Detavernier, and J. a. Martens, *J. Mater. Chem.*, 2011, **21**, 7692
67 C. Detavernier, J. Dendooven, S. P. Sree, K. F. Ludwig, and J. a Martens, *Chem. Soc. Rev.*, 2011, **40**, 5242–5253
68 J. Dendooven, S. P. Sree, K. De Keyser, D. Deduytsche, J. A. Martens, K. F. Ludwig, and C. Detavernier, *J. Phys. Chem. C*, 2011, **115**, 6605–6610
69 J. Dendooven, R. K. Ramachandran, K. Devloo-Casier, G. Rampelberg, M. Filez, H. Poelman, G. B. Marin, E. Fonda, and C. Detavernier, *J. Phys. Chem. C*, 2013, **117**, 20557–20561
70 J. Dendooven, B. Goris, K. Devloo-Casier, E. Levrau, E. Biermans, M. R. Baklanov, K. F. Ludwig, P. Van Der Voort, S. Bals, and C. Detavernier, *Chem. Mater.*, 2012, **24**, 1992–1994

Journal of Materials Chemistry A Accepted Manuscript

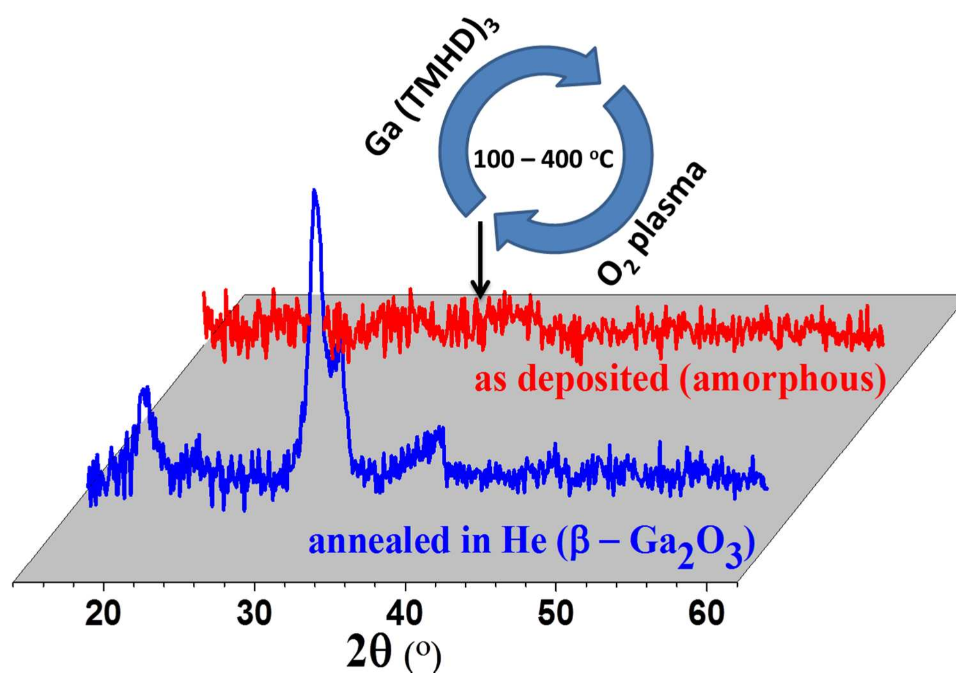

We demonstrate an ALD process for Ga_2O_3 that relies upon sequential pulsing of tris(2,2,6,6-tetramethyl-3,5-heptanedionato)gallium(III), [$Ga(TMHD)_3$] and O_2 plasma and enables the deposition from temperatures as low as 100 °C.

Journal of Materials Chemistry A Accepted Manuscript